

RESEARCH

Open Access



Coastal stressors reduce crop yields and alter soil nutrient dynamics in low-elevation farmlands

Jarrod O. Miller^{1*}, Patricia Ramalho de Barros², Alison N. Schulenburg² and Katherine L. Tully²

*Correspondence:

Jarrod O. Miller
jarrod@udel.edu

¹Department of Plant and Soil Sciences, College of Agriculture and Natural Resources, University of Delaware, Newark, DE, USA

²Department of Plant Science and Landscape Architecture, College of Agriculture and Natural Resources, University of Maryland, College Park, MD, USA

Abstract

Saltwater intrusion (SWI) driven by sea level rise (SLR) is transforming coastal agricultural fields along the Eastern Seaboard of the United States. In these regions, salinization is an increasing challenge for farmers, yet practical experience and effective management strategies for saline soils remain limited. To assess crop performance and nutrient dynamics under SWI, we conducted a four-year crop rotation, including sorghum (*Sorghum bicolor*), barley (*Hordeum vulgare*), and chloride-excluding (CE) soybean (*Glycine max*) across three SWI-affected farms and one no-salt site on the Lower Eastern Shore of Maryland, USA. We showed that sorghum exhibited the highest resilience to SWI of the evaluated crops, maintaining relative yields above 0.50, with better germination and survival under stress conditions, including drought, soil saturation, and herbivory. For all crops, yields increased with distance from the tidal waters, but barley frequently failed under saturated winter soils and soybean had more instances of zero yields in the plots. We found a strong inverse relationship between elevation above mean sea level (eMASL) and elevation relative to mean higher high water (eMHHW) and soil electrical conductivity (EC). Whereby soil EC increased exponentially below 0.75 m eMASL and 0.63 m eMHHW indicating key thresholds for crop success in low-lying coastal agricultural areas. Available soil phosphorus (P), ammonium (NH₄⁺), and nitrate (NO₃⁻) pools decreased over time in SWI-affected plots, whereas this decline was not observed at the no-salt site. Losses of P were up to 50% of the initial concentration. Our findings underscore the vulnerability of low-elevation coastal farmland to yield and nutrient loss and highlight the need for long-term adaptation strategies, including salt-tolerant crops and alternative land-use planning, to maintain agricultural viability in these transitional landscapes.

Keywords Coastal agriculture, Salinity, Saltwater intrusion, Sorghum, Soybean

1 Introduction

The accumulation of soluble salts in landscapes can reduce plant growth by reducing soil health and inducing stress [1, 2]. Soil salinization limits water uptake through osmotic stress in plants, and excessive ions, such as sodium (Na⁺), can cause plant toxicity [2, 3].



© The Author(s) 2025. **Open Access** This article is licensed under a Creative Commons Attribution-NonCommercial-NoDerivatives 4.0 International License, which permits any non-commercial use, sharing, distribution and reproduction in any medium or format, as long as you give appropriate credit to the original author(s) and the source, provide a link to the Creative Commons licence, and indicate if you modified the licensed material. You do not have permission under this licence to share adapted material derived from this article or parts of it. The images or other third party material in this article are included in the article's Creative Commons licence, unless indicated otherwise in a credit line to the material. If material is not included in the article's Creative Commons licence and your intended use is not permitted by statutory regulation or exceeds the permitted use, you will need to obtain permission directly from the copyright holder. To view a copy of this licence, visit <http://creativecommons.org/licenses/by-nc-nd/4.0/>.

While sources of soil salinity can include soil parent materials and agricultural irrigation in arid regions [4], coastal landscapes in humid regions are experiencing salinization through sea level rise (SLR) and saltwater intrusion (SWI) [5–7].

Salinization of coastal landscapes can be caused by multiple vectors, including salt sprays, stormwater surges, or nuisance flooding [7, 8]. However, due to SLR, the salinization front is moving further into coastal agricultural fields. This can occur in fields adjacent to tidal creeks, but also due to tidal or stormwater driven surges following drainage ditches [6, 9]. There are strong indicators that SWI is a growing problem worldwide [7, 10], with a doubling in salt patches on agricultural fields in the Delmarva (Delaware-Maryland-Virginia) Peninsula between 2011 and 2017 - a period of only 6 years [11]. The Delmarva Peninsula features extensive low-lying agricultural land, much of it less than 4 m above sea level, which increases its vulnerability to saltwater intrusion and flooding [5, 11].

Coastal salinization driven by sea level rise and tidal flooding poses serious agricultural challenges not only in the United States but also in regions such as South and Southeast Asia, including Bangladesh, India, and Indonesia, where monsoon-driven saltwater intrusion reduces crop yields and raises production costs [7]. Similar long-term impacts from storm surges, tropical storms, and tsunamis have been documented globally, including in Chile and the US Gulf Coast [Texas and Louisiana], highlighting the widespread and complex nature of saltwater intrusion effects on agriculture [7]. While heavy rainfall can mitigate salinity in some areas, low-lying and low-relief landscapes often experience prolonged recovery times and persistent productivity losses.

Along the eastern seaboard of the U.S., salinization is a growing issue for farmers, and there is limited experience with the management of saline and sodic soils. Ocean sprays and brackish waters can contain multiple ions including chloride (Cl^-), sodium (Na^+), potassium (K^+), magnesium (Mg^{2+}), calcium (Ca^{2+}), and sulfate (SO_4^{2-}) that may be deposited in fields [12], similar to soils forming in arid climates on marine parent materials [4]. These waters are typically dominated by Cl^- and Na^+ , though K^+ , Mg^{2+} , and Ca^{2+} are also present [13]. Within the Chesapeake Bay, salinity and ionic composition vary spatially, decreasing from the southern mouth to the headwaters, with seasonal peaks in late fall near Solomons, MD [14, 15]. Field management techniques for saline and sodic soils include tile drainage, deep tillage, and chemical amendments using Ca^{2+} [16], however these recommendations have largely been designed for climates that are drier than the Delmarva region. Due to lack of regional guidance or research in salinity management, field abandonment and retreat are a forced option that farmers must consider [17, 18]. However, farmers may also consider planting crops with a higher salt tolerance or the potential to exclude Cl^- [17, 19, 20].

In the Mid-Atlantic, corn (*Zea mays*), soybean (*Glycine max*), and winter small grains such as wheat (*Triticum aestivum*) or barley (*Hordeum vulgare*) are grown in rotations or double crop systems [21], used as feed for the regional poultry industry [22, 23]. The rotation of these grain crops is not designed around SWI, but rather drought tolerance under rainfed conditions (e.g. sorghum), reduced need for N fertilizer on soybean, and current grain prices. Of the crops grown in the Mid-Atlantic, irrigated barley has the strongest crop tolerance (based on the modified discount response function), where 50% of the crop yield (C_{50}) can be maintained at a saturated paste electrical conductivity (EC_e) of 17.53 dS m^{-1} [24], compared to irrigated wheat (5.85 ds m^{-1}), corn (5.54

ds m^{-1}) or soybean (7.16 ds m^{-1}). In recent years, grain sorghum has also increased in planting acreage across the Mid-Atlantic [22], with a salinity tolerance (C_{50}) slightly behind barley of 9.57 ds m^{-1} [24]. Crop salinity tolerance is also modeled using a modified discount response function based on electrical conductivity (ECe) thresholds at which yield begins to decline—such as 1.7 ds m^{-1} for corn, 5.0 for soybean, 6.0 for wheat, 6.8 for sorghum, and 8.0 for barley [25]. Additionally, although salinity tolerance for crops has been established, reduced effects of salinity on corn and soybean yields have been observed on finer textured soils [2]. Under these field conditions, corn and soybean did not see 50% yield reductions until 9.68 and 7.04 ds m^{-1} , respectively [2]. The type of salinity also controls crop responses, where soybean is more tolerant to SO_4 based salinity than when Cl is the dominant anion [2].

Breeding for salt-tolerance is difficult because it is a polygenetic trait [26, 27]. The chloride (Cl)-excluding (CE) soybean has been bred to resist the negative impacts of the Cl ion and can be purchased from seed dealers on the open market and are popular in arid regions where irrigation water tends to accumulate salts on soil surfaces [28]. In a controlled environment experiment, CE soybean germination declined under saline conditions mainly due to osmotic stress rather than ionic stress, suggesting that these cultivars are more sensitive to reduced water availability than to the presence of sodium and chloride [28]. In humid regions such as the Delmarva where fields are frequently inundated with saline waters, but also experience prolonged drought, this physiological limitation may reduce the suitability of CE soybeans in resilient crop rotations.

Salinity in coastal fields can affect crops in different ways, depending on the type of salt, soil characteristics, and water conditions. Although salt tolerance differs among crops, there is still limited guidance to help farmers choose the best rotations in areas affected by saltwater intrusion. Considering the varying responses of crops to salinity based on soil and ions present, as well as the variability in saline and brackish water concentrations, an examination of grain crop rotations for the Delmarva is needed. This study examined a rotation that included barley, sorghum, and Cl-excluding soybean to determine its success in coastal fields.

2 Materials and methods

2.1 Study sites

For this study, three rainfed agricultural fields along the Chesapeake Bay coastline were selected to examine the effects of SWI on a grain crop rotation (Fig. 1). We also established plots at Poplar Hill Lower Eastern Shore Research and Education Center (LES-REC) managed by the University of Maryland in Wicomico County, MD, which is not affected by saltwater intrusion (no-salt site).

Two fields were in Somerset County, MD (Farm 1 and Farm 3) and one site in Dorchester County, MD (Farm 6). In two of the fields (Farm 3 and Farm 6), farmers had previously abandoned approximately 0.73 ha and 0.47 ha, respectively, of the lower-elevation field edges bordering tidally influenced wetlands due to saltwater intrusion and reduced crop viability. In contrast, Farm 1 had an area of about 0.33 ha near the wetland edge where saltwater intrusion had caused reduced crop growth and emergence, but this area remained under active management and was not abandoned. The extent of abandonment reflects the varying histories and farmer responses to salinization in the region. Farm 3, historically cultivated since the 1950s, shifted from vegetable and

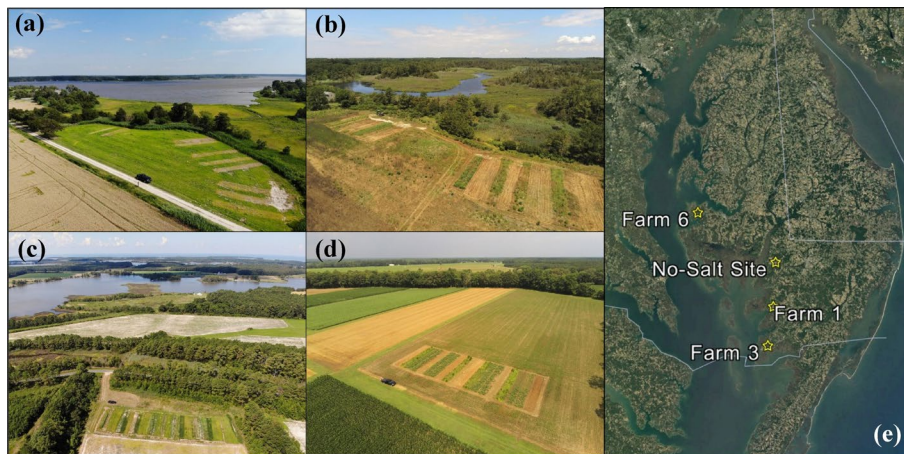


Fig. 1 Drone imagery of Farm 1 (a), Farm 3 (b), Farm 6 (c), the LESREC no-salt site (d), and their location along the Chesapeake Bay coastline in Maryland, USA (e)

Table 1 Established four-year crop rotation with three different entry points for sorghum, soybean and barley grain crops

Rotation	Year 1	Year 2	Year 3	Year 4
Entry Point 1	Sorghum	Barley/Soybean	Sorghum	Soybean
Entry Point 2	Sorghum	Soybean	Sorghum	Barley/Soybean
Entry Point 3	Soybean	Sorghum	Barley/Soybean	Sorghum

soybean production to sorghum in response to salt damage first observed in the mid-1990s. Farm 6 experienced severe flooding and salt damage following Superstorm Sandy in 2012, after which parts of the field were abandoned despite ongoing weed management. Farm 1 has been continuously farmed since the 1950s with periodic lime applications to mitigate soil conditions, and despite salt damage observed since 2000, it remains in production. Plots at Farm 3 and Farm 6 were established in 2018, while Farm 1 and the no-salt control site plots were established in 2019. Farms 1, 3, and 6 are adjacent to the tidally influenced Manokin River, East Creek, and Little Choptank River, respectively, all of which discharge into the Chesapeake Bay. See [18] for land use history information for each site.

2.2 Experimental design

Plots (3 m wide by 20 m long) were transects (Fig. 1) established as a randomized complete block design with six treatments, which included (1) fallow plots allowed to grow with weeds, (2) switchgrass (*Panicum virgatum*), (3) saltmarsh hay (*Spartina patens*), and 4–6) a four-year crop rotation with three different starting points (Entry point 1, Entry point 2, Entry point 3; Table 1). The rotation was designed as year 1: sorghum (*Sorghum bicolor*), year 2: winter barley (*Hordeum vulgare*) & double crop CI-excluding soybeans (*Glycine max*), year 3: sorghum, and year 4: full season CI-excluding soybeans (Table 1). We included three entry points to ensure focal crops were being grown in each field and each season for best comparison over time. These crops were selected based on their salinity tolerances, farmer suggestions, and regional options for grain markets. Plots were aligned perpendicular to the wetland or forested buffer edge associated with tidal salinity (Fig. 1). Four blocks were established, so that each site had 12 total grain crop plots within the three alternate crop starting points. Based on this design,

each block would alternate between two sorghum and one Cl-excluding soybean plot, and one sorghum and two Cl-excluding soybean plots every other year. Barley would be present in the study three out of four years (Table 1). Plots were placed directly adjacent and perpendicular to tidally influenced ditches or wetlands.

2.3 Field activities

Prior to planting both sorghum and soybean, glyphosate was sprayed at 4.7 L ha^{-1} as a pre-emergent application. Grain crops were then planted with a 1.52-m no-till Tye drill mounted by 3-point hitch to a John Deere tractor 6430. In year 1 (2018), sorghum and soybean were planted in 38-cm rows, but in subsequent years the spacing was narrower (19 cm). Due to the previous abandonment of two of the fields, the weed seed bank was greater, so that narrower rows were used to close the canopy and shade the weed seeding rates for sorghum were $198,000 \text{ seeds ha}^{-1}$ in 2018 and 2019 and raised to $296,526 \text{ seeds ha}^{-1}$ in subsequent years, based on University of Maryland recommendations. Soybean seeding rates were maintained at $457,144 \text{ seeds ha}^{-1}$ during the entire project while winter barley was drilled at $3,710,000 \text{ seeds ha}^{-1}$. Soybean varieties were chosen annually based on their chloride exclusion ranking but were different based on local availability. The Pioneer P42a52x soybean variety was planted in 2018–2019 while Pioneer P46A45PR was planted 2020–2022. The sorghum variety in 2018–2019 was Dekalb DKS 28-05 and Dekalb DKS 37-07 in 2020–2022. The barley variety remained Thoroughbred throughout the study, as a potential malting barley variety for the regional malting facility in Laurel, DE. Soybean plots were fertilized with K_2O based on a soil test and University of Delaware recommendations ($39\text{--}67 \text{ kg K ha}^{-1}$). Sorghum received 84 kg N ha^{-1} prior to planting as urea (46-0-0). Barley received urea-based N for a fall (30 kg N ha^{-1}) and spring (112 kg N ha^{-1}) applications. Seeding rates and fertilizer applications for each farm by year and treatment can be found in Supplemental Table 1.

Planting dates varied across seasons due to multiple external factors, including drought, soil saturation, and deer damage. These conditions, while unrelated to salinity, were unavoidable and sometimes intensified salinity effects (e.g., drought) or were typical of low-elevation coastal soils (e.g., saturation). Our strategy aimed to reduce confounding effects by replanting when emergence was severely limited.

In 2018, saturation and deer damage resulted in no emergence of sorghum or soybean planted in May, so replanting was performed in June. In 2019, drought and deer damage reduced emergence for the early June planting, and all plots were replanted two weeks later. The only other year plots were replanted was 2021, due to deer feeding, while in 2020 and 2022 plots were only planted once.

Barley plots were harvested in early June using a MiniBatt portable grain harvester from 0.5 m^2 sections of the plots. Sorghum plots were harvested in September the first season, but to reduce red wing black bird (*Agelaius phoeniceus*) feeding in plots we harvested in late August in 2019 and 2020 (all farms). In the following years, sorghum plots were covered with bird netting to reduce feeding. Within each sorghum plot, heads were harvested from three 1 m rows. The grain was removed, weighed, and then dried and tested for moisture. Soybean plots were harvested in mid-October from 0.5 m^2 sections in each plot. The grain was removed, weighed, and dried and tested for moisture content. At the no-salt site, plots were harvested with an Almaco Plot Combine. Phosphorus P concentrations [P] in grain samples were determined by grinding oven-dried

subsamples (60 °C) through a 2-mm mesh screen (Wiley Mill, Swedesboro, NJ), followed by digestion using a modified Kjeldahl method [29]. The digestate solution was analyzed for total P using colorimetry on a LACHAT QuikChem (LACHAT Instruments Loveland, CO) using the molybdate-blue method for PO₄-P (detection limit 0.01 mg PO₄-P/L; [30])

2.4 Soil sampling and analyses

A composite of three cores from the root zone was collected at depths of 0–10, 10–20, and 20–30 cm from each field site to determine baseline levels of soil nutrients and soil physical properties in March 2018 (Farm 3 and Farm 6) and November 2018 (Farm 1 and no-salt site). In subsequent years, soil samples were collected from each plot at depths of 0–10, 10–20, and 20–30 cm every November. All soil samples were collected using a 22-mm diameter push probe (AMS, Idaho Falls, ID, USA). A potassium chloride method was used to extract NH₄-N and NO₃-N from the soils and extracts were run on a LACHAT QuikChem (LACHAT Instruments Loveland, CO, USA). NH₄⁺-N and NO₃⁻-N concentrations were measured only in 2018 and 2020. In 2020, concentrations NH₄⁺-N and NO₃⁻-N were near zero or below the minimum detection limit of the colorimeter, so we discontinued measurements in subsequent years. Soil EC was measured in a 1:5 water extraction (wt: vol) on a Thermo Scientific Orion Versa Star Pro (Thermo Fisher Scientific, Hampton, NH, USA) and soil organic matter percentage was estimated using the loss-on-ignition method [31]. The Mehlich III method was used to extract bio-available phosphorus [32] and extracts were run on a LACHAT QuikChem (LACHAT Instruments Loveland, CO, USA) using the molybdate-blue method for PO₄-P (detection limit 0.01 mg PO₄-P/L; [30])

In 2018, soil bulk density cores were collected at 0–10 cm from each block at Farm 3 and Farm 6 using a 5-cm diameter x 15-cm deep core and an AMS compact slide hammer (Core Sampler Complete, AMS, American Falls, ID, USA). In 2019, soil bulk density cores were collected from each block at Farm 1 by digging 55-cm deep pits (50 cm²), where a 5-cm aluminum core was pushed horizontally into the side wall at 0–10 cm. In both cases, soils were dried at 105 °C for 7 days, and the dry weight of the soil was divided by the core volume to calculate bulk density (g cm⁻³). In 2021, soil bulk density was measured at the no-salt site using the same process as Farm 1. We calculated soil N and P pools by multiplying nutrient concentrations (mg kg⁻¹) by the depth of the sampled layer (10 cm) and the corresponding bulk density (g cm⁻³).

2.5 Drone imagery processing

Drone imagery was collected using a Micasense Altum multispectral camera mounted on a DJI Matrice 210 V2 drone for summer crops in August of each year. Imagery was processed using Pix4D Mapper and geo-corrected using ground control points that were marked in each field. Using Pix4D Mapper, vegetation indices were calculated, including normalized difference vegetation index (NDVI), green NDVI (GNDVI), normalized difference red edge index (NDRE), and visibly atmospheric resistance index (VARI). All indices maps were loaded into ArcGIS where polygon plot maps were created to extract average indices values.

2.6 Elevation data

We used two elevation metrics in this study: (1) elevation in meters above sea level (eMASL), and (2) elevation in meters above mean higher high water (eMHHW). The first metric provides absolute elevation of each plot relative to sea level, while the second estimates the relative elevation above the highest average daily tidal levels as an indicator of potential inundation. Elevation data was extracted from 1-meter digital elevation models (DEM) downloaded from Maryland iMAP (<https://imap.maryland.gov/>). To predict potential inundation, the mean high high water (MHHW) data later was downloaded from the National Oceanic and Atmospheric Administration (NOAA) Office for Coastal Management Webpage (https://coast.noaa.gov/slrdata/Tidal_Surfaces/index.html). For each plot, eMHHW was calculated by subtracting the NOAA MHHW surface value from the DEM derived elevation and are presented in Table 2.

2.7 Statistical analysis

Relative yields and vegetation indices as a randomized complete block design were compared using Proc GLM in SAS statistical software. Least square means were calculated with separation at an alpha level of 0.05. Soil $EC_{1:5}$ data from all SWI-affected farms were modeled against inverse elevation using a quadratic plateau model in SAS (PROC NLIN). Inverse elevation was used to emphasize the effect of lower elevation on $EC_{1:5}$. The model was fit across all sites to identify a threshold elevation below which $EC_{1:5}$ values increased non-linearly. The plateau breakpoint was interpreted as the elevation at which $EC_{1:5}$ begins to stabilize or decline.

We used a linear mixed-effects (LME) model (*lme4* package for R; [33]) to examine the effect of crop rotation on soil available P, NH_4^+ , NO_3^- , organic matter, and grain P. We analyzed each year and site individually with rotation (soybean and sorghum) as the main effects and block as the random effect. Soil P, NH_4^+ , NO_3^- , organic matter analyses were measured in year 1 (to understand baseline levels) and year 4 (after a full crop rotation). When a significant main factor was identified, pairwise comparisons were performed with Tukey's *post-hoc* test (function *glht*, package *multcomp*). All data were tested for normality using the Shapiro–Wilk test ($p < 0.05$). Where data failed the Shapiro–Wilk test, a Box–Cox transformation was performed to obtain a normal distribution of data [34]. Statistical analyses were performed using the R statistical software version 4.0 [35].

Table 2 Summary of average, minimum, and maximum elevation (m), $EC_{1:5}$, and the minimum and maximum elevation relative to mean higher high water (eMHHW) at the three sites affected by saltwater intrusion

Site	Distance from edge	Avg elevation (m)	$EC_{1:5}$ $dS\ m^{-1}$ (Min)	$EC_{1:5}$ $dS\ m^{-1}$ (Max)	Min eMASL (m)	Max eMASL (m)	Min eMHHW (m)	Max eMHHW (m)
Farm 1	5	0.73	0.06	1.49	0.59	0.83	0.29	0.53
Farm 1	15	0.82	0.06	0.83	0.75	0.89	0.45	0.59
Farm 1	20	0.87	0.05	0.78	0.80	0.91	0.50	0.61
Farm 3	5	0.76	0.07	2.99	0.72	0.86	0.41	0.54
Farm 3	15	0.77	0.03	2.11	0.71	0.89	0.39	0.58
Farm 3	20	0.79	0.03	1.40	0.68	0.97	0.36	0.65
Farm 6	5	0.66	0.10	1.22	0.61	0.70	0.41	0.49
Farm 6	15	0.69	0.08	1.01	0.63	0.72	0.42	0.51
Farm 6	20	0.71	0.12	0.66	0.68	0.74	0.47	0.54

3 Results

3.1 Effects of saltwater intrusion and elevation on soil EC and crop yields

At each SWI site, the highest $EC_{1.5}$ levels occurred at locations closest to the field edge (source of tidal flooding; Table 2). There were differences among sites, with the highest maximum $EC_{1.5}$ across all plots in Farm 3. Although Farm 6 has the lowest eMASL among the three farms, its $EC_{1.5}$ values are not consistently higher, suggesting that elevation alone does not explain soil salinity levels. However, when tidal influence is considered by adjusting with the elevation above mean higher high water (eMHHW), a different pattern emerges. Using this tidal elevation metric, Farm 1 and Farm 3 have lower eMHHW values than Farm 6, indicating a greater likelihood of tidal flooding and associated salt accumulation. This pattern is also evident in Fig. 2, where $EC_{1.5}$ measurements from Farm 6 begin to overlap those of Farm 1 only when using eMHHW rather than eMASL. Although Farm 3 plots were installed perpendicular to the tidal wetland, eMASL and eMHHW were lower toward the center of the field due to a slight

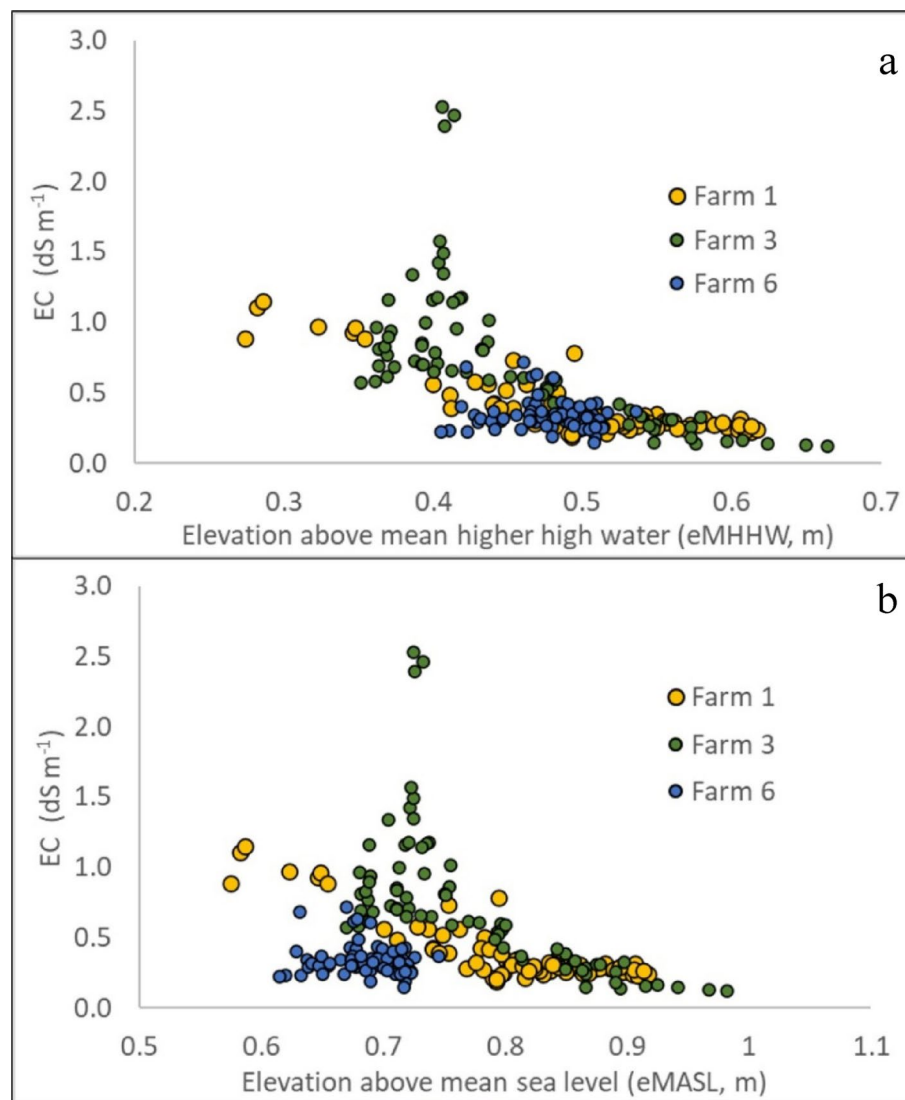


Fig. 2 Relationship between soil electrical conductivity (EC; $dS m^{-1}$) and **a** elevation related to tidal influences (eMHHW) and **b** absolute elevation in meters above mean sea level (eMASL) at three saltwater-intruded field sites on the Lower Eastern Shore of Maryland

depressional area (Table 2). Soil $EC_{1:5}$ was still highest closer to the tidal wetland in Farm 3.

Barley yields were only measured at Farm 1 and Farm 6, as the Farm 3 site never produced any final stands. Yields ranged from zero to 5908 kg ha^{-1} , which is lower than the Maryland statewide average of 6456 kg ha^{-1} [36], but higher than the maximum yield observed at the no-salt comparison site (4405 kg ha^{-1}). Barley plots with zero yield occurred at Farm 6 (2018–2019 season) and the no-salt site (2020–2021 season) as soils remained saturated and young barley plants did not survive the winter months. At Farm 1, yields were also zero for barley in the lowest elevation plots ($<0.70 \text{ m}$, $EC_{1:5} = 0.92$) with minimal plant survival during the 2020–2021 season. Although barley was planted over three seasons at Farm 3, no plants survived the winter in any year (Table 3).

Soybean yields ranged from 0 to 5126 kg ha^{-1} across all sites (Table 3). For comparison, statewide Maryland average soybean yields in 2023 were reported as 3161 kg ha^{-1} , while the highest yield recorded in the no-salt site during the study was 4974 kg ha^{-1} . At Farm 3, plots closest to the tidal wetland (5 m from edge) had zero yield (or growth/germination), unless the plots were above 0.8 m eMASL. The Farm 1 site only recorded yields of zero at the lowest eMASL, although deer feeding and drought caused total losses in 2019

Table 3 Summary of yield (minimum and maximum) and relative yield (minimum and maximum) by crop (barley, soybean, sorghum), site, and distance from the tidal ditch or wetland edge

Site	Distance from edge m	Yield (Min) kg ha^{-1}	Yield (Max)	Relative Yield (Min)	Relative Yield (Max)
Barley					
Farm 1	5	0.0	3477.35	0.00	0.58
Farm 1	15	732.8	5908.25	0.14	1.00
Farm 1	20	1143.3	4936.76	0.23	1.00
Farm 6	5	0.0	344.86	0.00	0.15
Farm 6	15	289.9	1123.30	0.12	0.50
Farm 6	20	544.8	2266.59	0.24	1.00
No-salt site	-	0	4404.90	-	-
Soybean					
Farm 1	5	0.0	500.80	0.00	0.09
Farm 1	15	77.5	2907.33	0.02	0.57
Farm 1	20	757.7	5126.94	0.23	1.00
Farm 3	5	0.0	4170.64	0.00	0.92
Farm 3	15	0.0	4339.98	0.00	1.00
Farm 3	20	0.0	4506.19	0.00	1.00
Farm 6	5	60.8	2927.56	0.02	0.82
Farm 6	15	12.5	2849.87	0.04	1.00
Farm 6	20	0.0	3584.01	0.00	1.00
No-salt site	-	2128.5	4973.80	-	-
Sorghum					
Farm 1	5	35.5	1571.81	0.02	0.97
Farm 1	15	23.5	2846.99	0.02	1.00
Farm 1	20	0.00	3724.35	0.00	1.00
Farm 3	5	0.00	1685.61	0.01	0.58
Farm 3	15	18.96	3472.49	0.01	1.00
Farm 3	20	13.89	2698.67	0.03	1.00
Farm 6	5	5.82	2607.94	0.00	0.76
Farm 6	15	26.00	3860.14	0.02	1.00
Farm 6	20	52.37	4960.70	0.02	1.00
No-salt site	-	3132.5	6052.0	-	-

and 2020 across all plots, potentially when adjacent *Phragmites australis* (an invasive reed species) would short-circuit the electric fence. Similar to barley, soybean germination and survival was limited, and likely related to multiple issues that could not be easily controlled in this field study, including saturation, drought, salinity, and deer foraging.

Sorghum yields ranged from zero to 4961 kg ha⁻¹ at the salt-affected sites (Table 3), while yields at the no-salt site ranged from 3133 to 6053 kg ha⁻¹. Lower yields for sorghum were due to reduced survival and growth, with additional losses due to foraging by birds. This was reduced in subsequent years by placing bird netting over the plots. Of all three grain crops, sorghum was the most likely to germinate and survive in each plot under the combination of stressors found on coastal fields.

We measured EC_{1.5} in soil (0–10 cm) every November from all SWI-affected sites (Farm 1, Farm 3 and Farm 6; Fig. 2). The plots at Farm 6 had the smallest range in eMASL (0.61 to 0.74 m), but were lower compared to Farm 1 and Farm 3. Even with the lowest eMASL, Farm 6 did not have EC_{1.5} values as high as Farm 3, all remaining below 1.0 dS m⁻¹. While Farm 1 had lower elevations than Farm 3, the EC_{1.5} did not have as steep an increase with eMASL. In contrast, Farm 3 had an exponential increase in EC_{1.5} as elevation dropped below 0.8 m.

We modeled the natural log of soil EC_{1.5} (lnEC) as a function of the inverse of elevation above mean sea level (1/eMASL) using a quadratic plateau regression. The model follows the form $\ln(\text{EC}_{1.5}) = \alpha + \beta \times (1/\text{eMASL})$ up to a breakpoint, after which it levels off at a plateau value. The estimated parameters were $\alpha = -20.81$, $\beta = 29.87$, and the plateau at 1.33. This breakpoint corresponds to approximately 0.75 m eMASL, indicating that below this elevation, EC_{1.5} increases sharply, while above it, EC_{1.5} stabilizes. Similarly, we modeled average soil EC_{1.5} as a function of elevation relative to mean higher high water (eMHHW) using a quadratic plateau regression of the form $\text{EC}_{1.5} = \alpha + \beta \times \text{eMHHW}$ up to a breakpoint, followed by a plateau. The estimated parameters for this model were $\alpha = 3.03$, $\beta = -8.95$, and the plateau at 0.63, indicating that EC_{1.5} decreases sharply with increasing eMHHW until about 0.63 m, above which EC_{1.5} stabilizes.

These results suggest that lower elevations are more prone to flooding and saltwater exposure, leading to elevated EC_{1.5} values. The exponential increase in EC_{1.5} observed at Farm 3 as elevation dropped below 0.8 m supports this, as lower-lying areas are more frequently inundated by saltwater or retain salts for longer periods. The consistent observation of increased EC_{1.5} below 0.75 m eMASL and 0.63 m eMHHW across all sites reinforces the importance of these elevation thresholds in controlling soil salt accumulation.

3.2 Relative yields by crop and averaged across crops

At each site, relative crop yield (Table 3) was lowest closest to the field edges (0–5 m), which were often the lowest elevations and closest to the saltwater sources (saline ditch; Table 2). The highest maximum relative yield was always recorded >5 m from the field edge. Yields were 18 to 28% of their maximum measured at each site at the lowest elevation, while they were 39 to 53% of the maximum yield from 5 to 20 m from the field edge (Table 4). When yields were compared to no-salt site averages of each crop, the lowest elevations were 13–22% of the maximum, and 24–46% above that. However, they were only significantly different by distance from the field edge at the Farm 1 and Farm 6 sites.

Table 4 Relative yields by site based on distance from the field edge averaged across all crops, yields relative to the no salt-site, and drone derived vegetation indices, including normalized difference vegetation index (NDVI), green NDVI (GNDVI), normalized difference red edge index (NDRE), and the visible atmospherically resistant index (VARI)

Distance from edge (m)	Relative yield	Relative to no-salt site	NDVI	GNDVI	NDRE	VARI
Farm 1						
5	0.18 b	0.14 b	0.53 b	0.53 a	0.29 b	0.09
15	0.43 a	0.44 a	0.65 a	0.61 a	0.37 a	0.21
20	0.43 a	0.46 a	0.63 a	0.60 a	0.36 a	0.18
<i>p-value</i>	< 0.0001	< 0.0001	0.049	0.0211	0.0338	0.1973
Farm 3						
5	0.23 b	0.13	0.64 b	0.54	0.25	0.33 b
15	0.39 a	0.25	0.75 a	0.62	0.33	0.51 a
20	0.43 a	0.24	0.78 a	0.62	0.31	0.57 a
<i>p-value</i>	0.0212	0.1559	< 0.0001	0.0112	0.2089	< 0.0001
Farm 6						
5	0.28 b	0.21 b	0.68	0.5846	0.30	0.20
15	0.46 a	0.32 a	0.69	0.6014	0.33	0.20
20	0.53 a	0.38 a	0.68	0.5944	0.31	0.19
<i>p-value</i>	< 0.0001	0.0056	0.9188	0.7012	0.6831	0.9845

Table 5 Relative yields where absolute elevation for each grain crop where absolute elevation (eMASL) was less than 0.75 m and elevation relative to tidal inundation (eMHHW) was less than 0.63

	eMASL	eMHHW
Sorghum	0.42 a	0.38
Soybean	0.33 b	0.35
Barley	0.28 b	0.39
<i>p-value</i>	0.0454	0.5562

Drone measurements had similar patterns, where they estimate ground cover through multispectral sensors [37]. The NDVI and GNDVI measurements were significantly different at Farm 1 and Farm 3 sites, with lower values observed in plots 5 m from the field edge, indicating reduced growth. The NDRE was only lower 5 m from the edge at Farm 1 5 m and VARI at Farm 3 (Table 4). Despite differences in relative yield at Farm 6, none of the drone-derived vegetation indices showed significant variation from the field edge (Table 5).

Using elevation thresholds derived from a quadratic plateau regression of $EC_{1:5}$ across all sites (with inflection points at 0.75 m for eMASL and 0.63 m for eMHHW, as described above), we specifically examined relative crop yields at locations below these thresholds and found that yield responses varied by species. Sorghum maintained the highest relative yield under lower elevation conditions (0.42 under eMASL and 0.38 under eMHHW), while barley and soybean yields performed poorly at low elevations. Barley and soybean yields were significantly lower than sorghum yields under eMASL (0.28 and 0.33, respectively). Differences were not significant under eMHHW ($p = 0.5562$), likely due to most yields still falling below this point.

3.3 Soil nitrogen and organic matter

Overall, topsoil (0–10 cm) ammonium-nitrogen (NH_4^+ -N) and nitrate-nitrogen (NO_3^- -N) pools declined in the saltwater-intruded field sites over the course of the study (from 2018 to 2020) (Fig. 3; $p < 0.05$). In contrast, NH_4^+ -N and NO_3^- -N concentrations

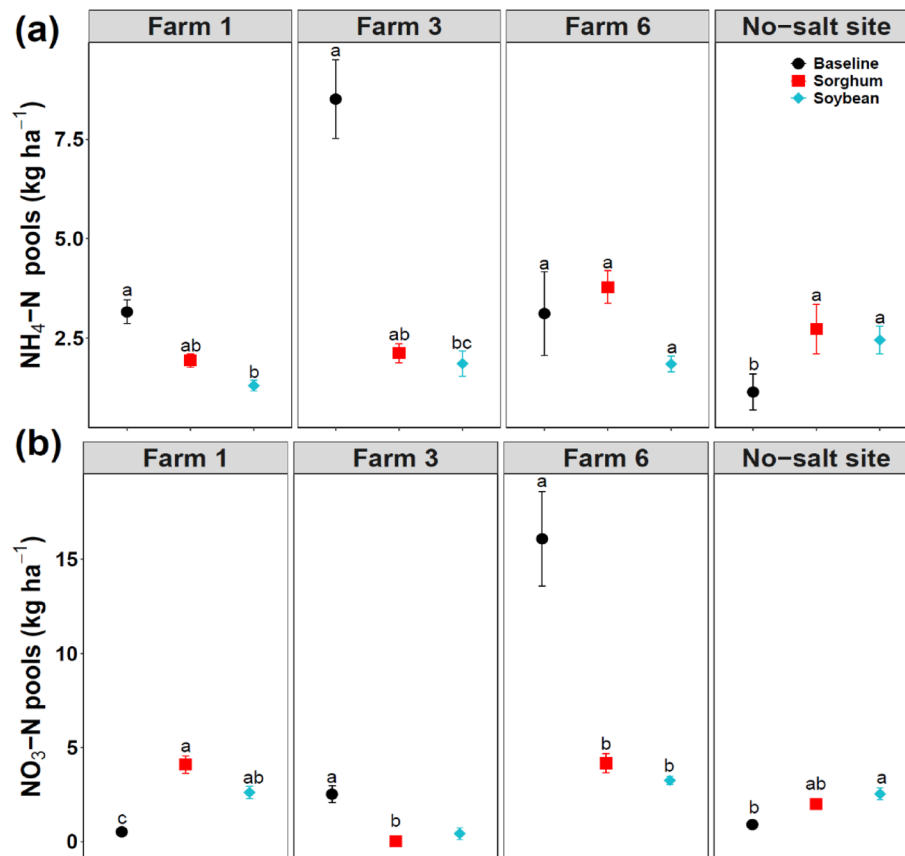


Fig. 3 a Ammonium-nitrogen ($\text{NH}_4^+\text{-N}$), and b nitrate-nitrogen ($\text{NO}_3^-\text{-N}$) pools in topsoil (0–10 cm) at three saltwater-intruded field sites and one no-salt site on the Lower Eastern Shore of Maryland, measured in 2018 (baseline) and 2020. Different letters indicate significant differences ($p < 0.05$) among crop rotation within each year and across years based on Tukey's *post-hoc* pairwise comparisons. Error bars are the standard error of the mean

increased at the no-salt site over the course of the study. Soil organic matter (0–10 cm) was relatively similar across sites (ranging from 2.0 to 4.5%), with a significant decrease over time only at Farm 1 (Figure S1; $p < 0.05$).

3.4 Soil and grain phosphorus concentrations

Available soil P pools in the topsoil varied across sites. We observed decreases in soil P pools from year 1 (baseline) to year 4 at Farm 3, Farm 6, and the no-salt site (Fig. 4; $p < 0.05$ in all cases), indicating that soils are losing P over time. At Farm 1, no significant differences were observed among years.

We found similar patterns in sorghum and soybean grain P concentrations among all saltwater-intruded sites in year 2 and year 4 with significantly higher P concentrations in soybean grains ($5.0\text{--}8.0 \text{ g kg}^{-1}$) than sorghum grains ($3.5\text{--}6.0 \text{ g kg}^{-1}$; $p = 0.01$ in all cases; Fig. 5a). Soybean grain P concentrations were highest at Farm 1 in year 4 compared to the other farms ($6.1\text{--}8.0 \text{ g kg}^{-1}$; $p < 0.001$). Finally, soybean grain P concentrations were lower ($4.5\text{--}5.5 \text{ g kg}^{-1}$) at the no-salt site than at the SWI-affected sites in year 4.

Sorghum grain P concentration was slightly higher than soybean grain in year 2 at Farm 6. There was no significant effect of treatment at Farm 3 in year 2. Since only sorghum was collected at Farm 3 and Farm 6 in year 4, we could not compare to soybean yields. Sorghum had the highest grain P stocks at Farm 1. At the no-salt site, soybean

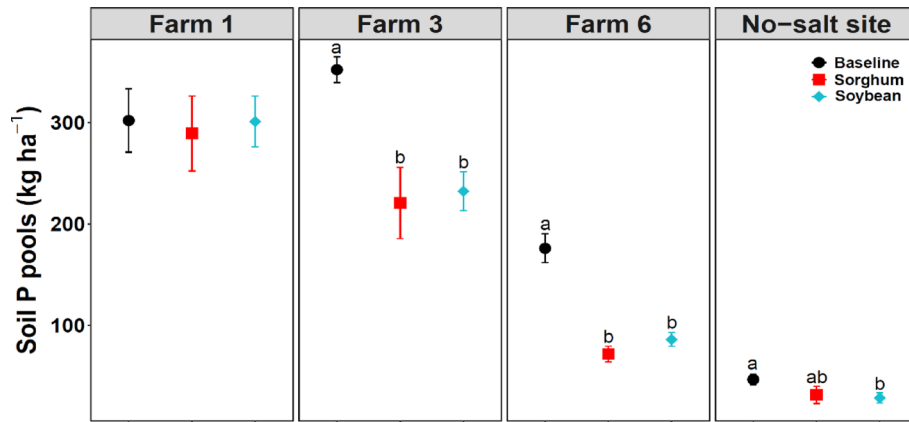


Fig. 4 Available soil P pools (kg ha^{-1}) in topsoil (0–10 cm) at three saltwater-intruded field sites and one no-salt site on the Lower Eastern Shore of Maryland, measured in year 1 (baseline) and year 4. Different letters indicate significant differences ($p < 0.05$) among rotations within each year and across years based on Tukey's *post-hoc* pairwise comparisons. Error bars are the standard error of the mean

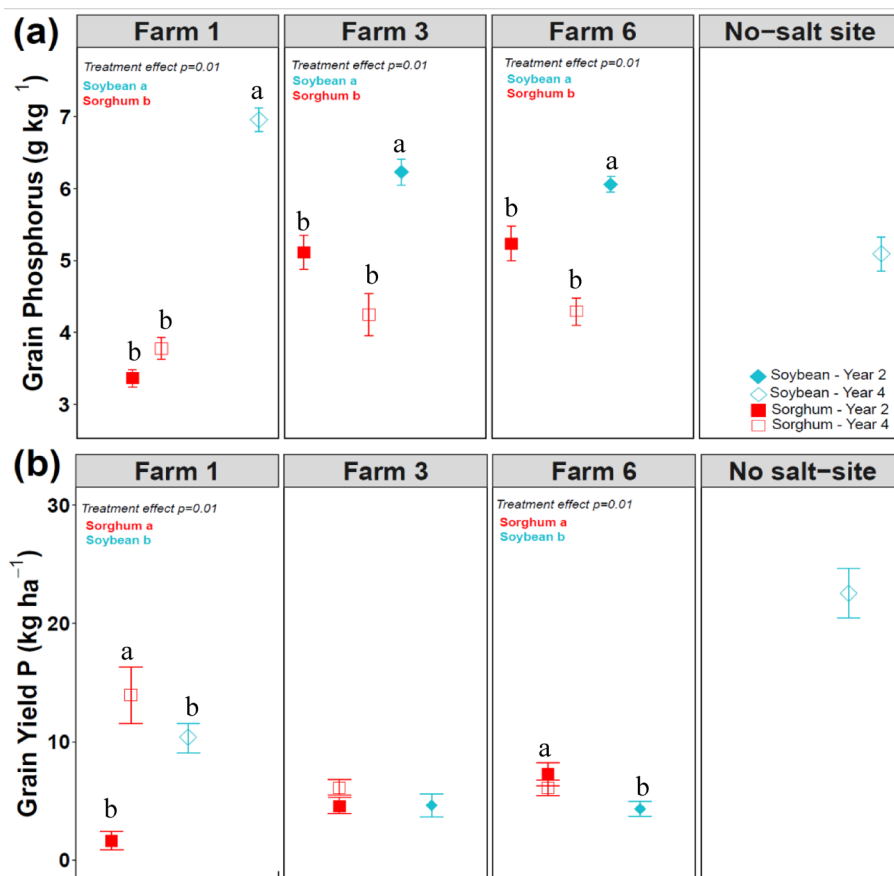


Fig. 5 **a** Grain P concentrations (g kg^{-1}) and **b** grain P stocks (kg ha^{-1}) at three saltwater-intruded field sites and one no-salt site on the Lower Eastern Shore of Maryland, measured in study years 2 and 4. Different letters indicate significant differences ($p < 0.05$) among rotations within each year and across years based on Tukey's *post-hoc* pairwise comparisons. Error bars are the standard error of the mean

grain P stocks were higher than pools in the SWI-affected sites (22.5 kg grain-P ha⁻¹; Figure 5b).

4 Discussion

Salinization in coastal regions is driven by SLR, increased frequency of storms and tidal flooding, drought, water extraction, and the connection of coastal farms to saline waters via ditches (Fig. 6; [5]). Salinization leads to elevated soil salinity and alters water and nutrient dynamics, limiting plant establishment and reducing yield (Fig. 6a; [17, 28, 38]). Salinization also accelerates marsh migration and coastal forest loss, which can displace wildlife such as deer and waterfowl, increasing herbivory pressure on nearby cropland (Fig. 6a–c). In our study, wildlife foraging was commonly observed, with deer entering fields from adjacent tidal creeks and wetlands (Fig. 6c). Compounding the issue, early-season drought, saturation, and/or salinity spikes have created inhospitable conditions for grain production (Fig. 6a). In response, farmers are seeking adaptation strategies that include changes in crop selection and field management. Our study shows that sorghum provides the best resilience to the direct and indirect effects of salinization and should be considered as a transitional crop in the coastal zone.

4.1 Sorghum provides greatest resilience to salinization

Among the three crops evaluated, sorghum demonstrated the highest resilience across all field conditions, including herbivore foraging, drought, and salinity. Sorghum was the only crop that had relative yields greater than 0.50 in the 5 m plots and had higher relative yields than CE soybean and barley at elevations <0.75 eMASL. Unlike barley and CE soybean, sorghum successfully germinated under marginal moisture conditions and maintained yield stability even in areas affected by moderate salinity and herbivory. Regardless of deer foraging, soybean only germinated and survived under ideal conditions, while barley frequently failed during wet winters and under soil saturation.

Although CE soybean and barley are generally reported to tolerate higher salinity thresholds than sorghum, with yield declines typically beginning at 10 and 8.0 dS m⁻¹, respectively, compared to 6.8 dS m⁻¹ for sorghum [39] our results showed that sorghum was the most resilient crop under field conditions. This outcome may be explained by the presence of multiple interacting stressors, such as periodic waterlogging, poor soil

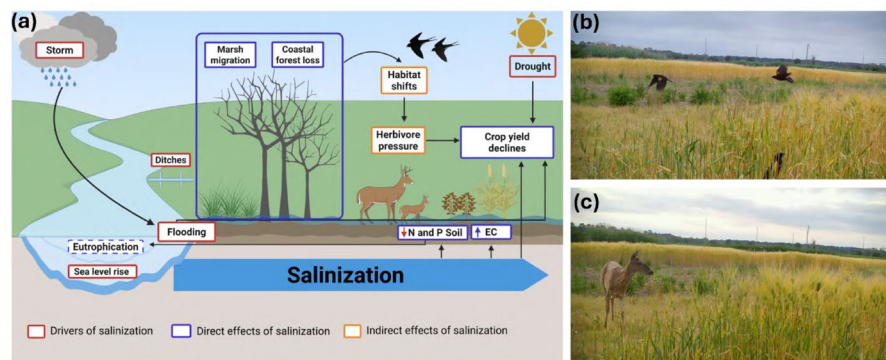


Fig. 6 **a** Conceptual diagram of drivers of salinization (red boxes), direct effects of salinization (blue boxes) and indirect effects (yellow boxes) of salinization in coastal regions. **b** Red-winged black bird (*Agelaius phoeniceus*) forages on barley on Farm 1. **c** A white-tailed deer (*Odocoileus virginianus*) stands in a barley plot after crossing through electric fencing to consume grain on Farm 1

aeration, and early-season drought, which are common in humid coastal regions like Delmarva. As a C4 plant, sorghum possesses key traits such as high photosynthetic efficiency, strong tolerance to diverse abiotic stresses, and the ability to maintain high biomass production under adverse conditions [40–42]. These results underscore sorghum's superior performance in vulnerable low-lying coastal zones.

4.2 Topographic gradients drive yield responses

We found that relative yields increased with distance from the source of saltwater (> 5 m from the field edge, which is likely related to subtle elevation gains, which reduce soil salinity (0.75 m eMASL or 0.63 eMHHW; Table 2). It is important to note that these are very small changes in elevation < 1 m, which can have a huge impact on crop productivity, and leaves farmers fighting for inches in coastal agroecosystems. Although outside the scope of this study, we observed flooding to be more pronounced in lower elevation areas (Fig. 7). Similar patterns were reported in agricultural fields on Maryland's Eastern Shore [43]. Higher elevation fields were more likely to remain in production with salt-sensitive crops, while lower elevation areas (below 2 m eMHHW) more frequently transitioned to salt-tolerant species or converted to wetlands due to increased vulnerability to salinity and tidal inundation [43]. However, elevation alone does not explain these lower yields, as Farm 3 had lower eMASL and eMHHW further from the edge, perhaps because herbivore foraging is more likely to occur on the edges of fields. Therefore, it is likely that both direct (salinity) and indirect (herbivore pressure) led to yield declines in coastal farms.

Site-level differences also played a significant role in yield variability. At Farm 3, despite higher overall salinity, mid-elevation plots produced relatively high soybean yields when soil and growing conditions were more favorable. In contrast, Farm 6 had



Fig. 7 Example of flooding in a low-elevation area of a coastal agricultural field (Farm 1) on the Lower Eastern Shore of Maryland adjacent to the Manokin River

relatively low EC values, indicating that other factors, such as inadequate drainage, may have reduced yields at these sites. Poor drainage and excess soil water can severely limit root development and nutrient uptake in soybeans by reducing oxygen availability in the root zone and impairing physiological processes, which compromises plant growth and productivity [44, 45].

Finally, although most yields from SWI-affected fields were a fraction of the average no-salt site yields, it is important to note that our focal plots were located in some of the least productive regions of the field. At both Farm 3 and Farm 6, farmers provided access to previously abandoned areas. Therefore, the poor yields observed here, when considering the effects of SWI, likely represent a worst-case scenario. Smaller fields with boundaries adjacent to tidal creeks or brackish shorelines may face even greater challenges, as they have a higher proportion of land exposed to saltwater intrusion [9]. Moreover, the observed relationship between EC and elevation (Fig. 2) suggests that even larger fields with gentle slopes may face increasing risk of yield decline as saltwater continues to migrate inland.

4.3 Saltwater intrusion alters nutrient dynamics

Our study showed that SWI influenced soil nutrient dynamics. From 2018 to 2020, concentrations of NH_4^+ and NO_3^- declined significantly at SWI-affected sites. In many of the samples analyzed, NH_4^+ and NO_3^- concentrations were nearly zero in 2020. In contrast, NH_4^+ and NO_3^- concentrations increased at the no-salt site in 2020 compared to baseline levels. This decline in inorganic N at SWI-affected sites may be attributed to several mechanisms driven by increased soil salinity. First, saline conditions expose microbial communities to osmotic and ionic stress, which can reduce enzyme efficiency and microbial biomass and inhibit the decomposition of organic matter. Reduced decomposition rates can cause a substantial decline in the pool of potentially mineralizable N [46, 47]. Additionally, SWI can alter the soil's redox environment by promoting anoxic conditions that enhance denitrification, whereby NO_3^- is reduced to gaseous forms such as N_2 or N_2O , resulting in nitrogen losses from the system [48, 49]. Furthermore, in SWI-affected areas, NH_4^+ bound to negatively charged soil surfaces can be displaced by divalent cations found in saltwater, including Na^+ , Ca^{2+} , and Mg^{2+} , particularly under high ionic strength conditions [17, 50, 51]. This displacement releases NH_4^+ into the soil solution, increasing its mobility. Once in solution, NH_4^+ concentrations can move downstream via tidal exchange or storm-driven runoff through ditch networks, where the exported N may contribute to nutrient pollution in downstream watersheds [51].

We observed a decline in soil available P pools over time at all sites except Farm 1. The reduction in soil P was more pronounced in the SWI-affected sites than at the no-salt site, despite the fact that crop productivity in the SWI plots was the lowest. Moreover, P removed in harvested grains was relatively low and did not account for the magnitude of P depletion observed in the soil over the course of the study (Fig. 8). These results suggest that the decline in soil P in SWI-affected sites was not primarily due to crop uptake and removal, but instead linked to leaching losses driven by saltwater-induced changes in soil chemistry. In SWI-affected environments, sulfate (SO_4^{2-}) introduced through SWI can displace phosphate (PO_4^{3-}) from soil mineral surfaces, particularly those associated with iron oxides [17, 52]. This displacement is intensified under low-oxygen (anoxic) conditions, which are common in saturated or poorly drained soils.

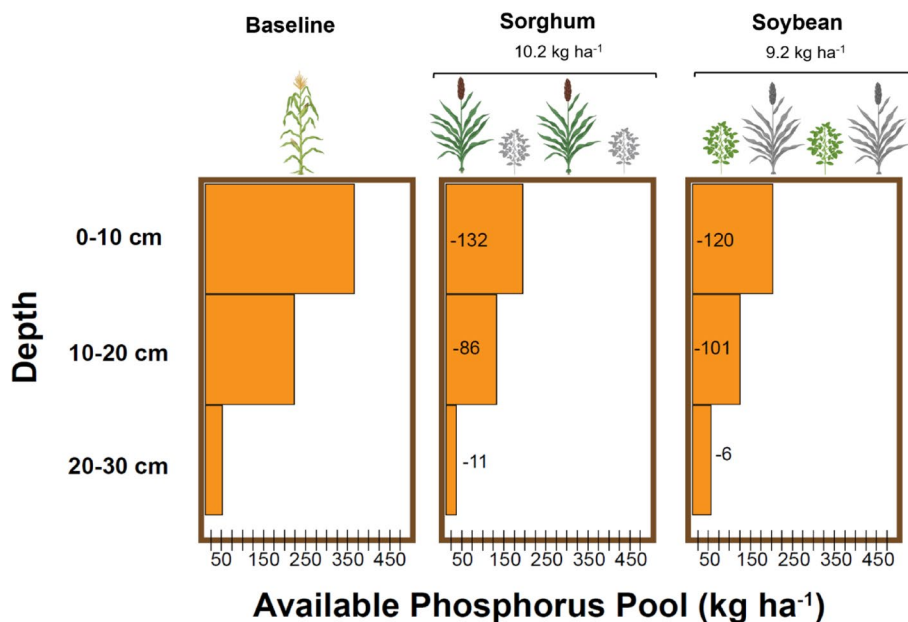


Fig. 8 Conceptual diagram illustrating total grain phosphorus (P) and corresponding belowground available P pools at three soil depths (0–10, 10–20, and 20–30 cm) under rotations at Farm 3. Baseline values (Year 1) are compared to Year 4. Changes in available P from Year 1 to Year 4 are represented as values inside the bars, where positive numbers (+) indicate an increase in P pools and negative numbers (-) indicate a decrease over time

Under such conditions, iron (Fe^{3+}) minerals are reduced to Fe^{2+} , which diminishes PO_4^{3-} sorption capacity and increases its mobility in the soil solution, thereby enhancing its susceptibility to leaching [17, 53]. This can contribute to nutrient runoff and eutrophication in nearby water bodies [54, 55], a significant environmental concern as it promotes algal blooms, depletes oxygen levels, and harms aquatic life [56]. To address these risks, incorporating restoration species such as *Panicum virgatum*, *Spartina patens*, and *Trip-sacum dactyloides*, which are known to tolerate salinity, may offer a sustainable strategy to mitigate phosphorus runoff in SWI-affected areas [18, 57].

Our study demonstrates that crops in saltwater intrusion-affected coastal zones face multiple interacting stressors, including elevated salinity, drought, saturation, poor drainage, and increased herbivory pressure from wildlife such as deer. These compounding challenges reduce crop establishment and yield, complicating management decisions for farmers. The findings underscore the importance of local agricultural and environmental agencies incorporating these complex stressors into their outreach and support programs, including guidance on soil amendments and drainage improvements. Future research will expand crop resilience trials and investigate integrated management practices, such as salt-tolerant cultivars, soil amendment strategies, conservation species, and improved drainage. Given the trajectory of sea-level rise and climate variability, coastal farming communities must proactively adopt adaptive strategies to maintain agricultural productivity and ecosystem health in these increasingly vulnerable landscapes.

5 Conclusions

Saltwater intrusion is moving through coastal landscapes across the Eastern Seaboard and the Mid-Atlantic region of the U.S. Our study highlights the resilience of sorghum under a range of stress conditions—including salinity, drought, and wildlife pressure—making it a promising option for coastal fields affected by saltwater intrusion. We also

observed a clear yield threshold linked to elevation, with relative yields increasing above 0.73 m above sea level. Below this elevation, yields declined sharply, suggesting that continued crop production in these low-lying zones may no longer be viable. To better assess risk, measurements of salinity as $EC_{1:5}$ should incorporate elevation relative to mean higher high water (eMHHW) as a reference, since tidal influences vary across the Delmarva Peninsula even where field elevations are similar.

Nutrient dynamics further underscore the vulnerability of low-elevation zones to saltwater intrusion. Across SWI-affected sites, we observed steep declines in inorganic nitrogen (NH_4^+ and NO_3^-) and available P over time, driven by salinity-induced changes in microbial activity, soil redox conditions, and nutrient displacement. This underscores the need for restoration species which may survive these conditions, providing nutrient uptake and a buffer along field edges.

Supplementary Information

The online version contains supplementary material available at <https://doi.org/10.1007/s44279-025-00303-7>.

Additional file 1

Acknowledgements

We would like to acknowledge Shawn Tingle for plot planting and management and our farmer and landowner cooperators for accessing their fields.

Author contributions

J.M, P.B, A.S., and K.T. wrote the manuscript text. J.M., P.B. and A.S. prepared the figures. All authors reviewed and edited the manuscript.

Funding

This research was funded by the United States Department of Agriculture *National Institute of Food and Agriculture* (NIFA) [2018–68002–27915] and Chesapeake Bay Stewardship Fund—Small Watershed Grant from the National Fish and Wildlife Foundation partnership with the U.S. Environmental Protection Agency (Award No. 0603.20.071142).

Data availability

All data supporting the findings of this study are available within the paper and its Supplementary Information.

Declarations

Ethics approval and consent to participate

Not applicable.

Consent for publication

Not applicable.

Competing interests

The authors declare no competing interests.

Received: 18 June 2025 / Accepted: 28 July 2025

Published online: 04 August 2025

References

- Westhoff S, Clay DE, Osterloh K, Clay SA, DeSutter TM, Nleya T, Ferreira JF, Suarez DL, Sandhu D. An introduction to salinity and sodicity. Salinity and sodicity: A growing global challenge to food security. *Environmental Quality and Soil Resilience*; 2024.
- Butcher K, Wick AF, DeSutter T, Chatterjee A, Harmon J. Soil salinity: A threat to global food security. *Agron J*. 2016;108(6):2189–200. <https://doi.org/10.2134/agronj2016.06.0368>.
- Clay DE, DeSutter TM, Clay SA, Nleya T. Salinity and sodicity: A growing global challenge to food security, environmental quality and soil resilience. Wiley; 2024. p. 197.
- Westhoff S, Osterloh K, Malo D. Formation and classification of Salt-Affected soils. *Salinity and sodicity: A global challenge to food security. Environmental Quality and Soil Resilience*; 2024.
- Tully K, Gedan K, Epanchin-Niell R, Strong A, Bernhardt ES, BenDor T, et al. The invisible flood: the chemistry, ecology, and social implications of coastal saltwater intrusion. *Bioscience*. 2019;1(5):368–78. <https://doi.org/10.1093/biosci/biz027>.
- Kirwan ML, Michael HA, Gedan KB, Tully KL, Fagherazzi S, McDowell NG, Molino GD, Pratt D, Reay WG, Stotts S. Feedbacks regulating the salinization of coastal landscapes. *Annual Rev Mar Sci*. 2024. <https://doi.org/10.1146/annurev-marine-070924-031447>.

7. Miller J. An Introduction to Coastal Flooding Impact on Salinity and Sodidity in Agricultural Fields. In: Salinity and Sodidity: A Global Challenge to Food Security, Environmental Quality, and Soil Resilience. 2024.
8. Mofatkhari HR, AghaKouchak A, Sanders BF, Feldman DL, Sweet W, Matthew RA, et al. Increased nuisance flooding along the Coasts of the United States due to sea level rise: past and future. *Geophys Res Lett*. 2015;42(22):9846–52. <https://doi.org/10.1002/2015GL066072>.
9. Bhattachan A, Emanuel RE, Ardón M, Bernhardt ES, Anderson SM, Stillwagon MG, Ury EA, BenDor TK, Wright JP. Evaluating the effects of land-use change and future climate change on vulnerability of coastal landscapes to saltwater intrusion. *Elem Sci Anth*. 2018;6:62. <https://doi.org/10.1525/elementa.316>.
10. Huang M, Zhang Z, Sheng Z, Zhu C, Zhai Y, Lu P, et al. Soil salinity and maize growth under cycle irrigation in coastal soils. *Agron J*. 2019;111(5):2276–86. <https://doi.org/10.2134/agnonj2018.10.0684>.
11. Mondal P, Walter M, Miller J, Epanchin-Niell R, Gedan K, Yawatkar V, et al. The spread and cost of saltwater intrusion in the US Mid-Atlantic. *Nat Sustain*. 2023;6(11):1352–62. <https://doi.org/10.1038/s41893-023-01186-6>.
12. Du J, Hesp PA. Salt spray distribution and its impact on vegetation zonation on coastal dunes: a review. *Estuaries Coasts*. 2020;1(8):1885–907. <https://doi.org/10.1007/s12237-020-00820-2>.
13. Young EG, Smith DG, Langille WM. The chemical composition of sea water in the vicinity of the Atlantic provinces of Canada. *J Fish Res Board Can*. 1959;16(1):7–12.
14. Wells RC, Bailey RK, Henderson EP. Salinity of the water of Chesapeake Bay. 1929.
15. Beaven GF. Temperature and salinity of surface water at Solomons, Maryland. *Chesap Sci*. 1960;1(1):2–11.
16. Peterson AR, DeSutter TM, Daigh ALM, Meehan MA, Derby N. Effects of calcium amendments on hydraulic conductivity and sodium content of brine-impacted soils. *Agrosystems Geosci Environ*. 2024;7(3):e20556. <https://doi.org/10.1002/agg2.20556>.
17. Tully KL, Weissman D, Wyner WJ, Miller J, Jordan T. Soils in transition: saltwater intrusion alters soil chemistry in agricultural fields. *Biogeochemistry*. 2019;142(3):339–56. <https://doi.org/10.1007/s10533-019-00538-9>.
18. Schulenburg AN, Miller JO, Gedan KB, Weissman D, Tully KL. Management strategies for reducing phosphorus levels in saltwater-intruded agricultural fields. *Agric Ecosyst Environ*. 2024;15:370:109034. <https://doi.org/10.1016/j.agee.2024.109034>.
19. Abel GH. Inheritance of the capacity for chloride inclusion and chloride exclusion by soybeans. *Crop Sci*. 1969;9(6):697–8. <https://doi.org/10.2135/cropsci1969.0011183X000900060006x>.
20. Maas EV, Hoffman GJ. Crop Salt Tolerance—Current Assessment. *J Irrig Drain Div*. 1977;103(2):115–34. <https://doi.org/10.1061/JRCEA4.0001137>.
21. Jones BP, Holshouser DL, Alley MM, Roygard JKF, Anderson-Cook CM. Double-Crop soybean leaf area and yield responses to Mid-Atlantic soils and cropping systems. *Agron J*. 2003;95(2):436–45. <https://doi.org/10.2134/agnonj2003.4360>.
22. Balota M, Thomason WE, Mehl HL, Cahoon CW, Reay-Jones F, Taylor SV, et al. Revival of grain sorghum in the Mid-Atlantic. *Crops Soils*. 2018;51(1):32–47. <https://doi.org/10.2134/cs2018.51.0110>.
23. Duke JM, McGrath JM. An agronomic-economic approach to connect manure nutrients back to grain-producing regions. *J Environ Qual*. 2022;51(4):552–65. <https://doi.org/10.1002/jeq2.20329>.
24. Steppuhn HA, Van Genuchten MT, Grieve CM. Root-zone salinity: I. Selecting a product–yield index and response function for crop tolerance. *Crop Sci*. 2005;45(1):209–20. <https://doi.org/10.2135/cropsci2005.0209>.
25. Grieve CM, Grattan SR, Maas EV. Plant salt tolerance. *ASCE Man Rep Eng Pract*. 2012;71:405–59. <https://doi.org/10.1061/9780784411698.ch13>.
26. Flowers TJ, Flowers SA. Why does salinity pose such a difficult problem for plant breeders? *Agric Water Manag*. 2005;15(1):15–24.
27. Flowers TJ, Galal HK, Bromham L. Evolution of halophytes: multiple origins of salt tolerance in land plants. *Funct Plant Biol*. 2010; 2;37(7):604–12.
28. de la Reguera E, Veatch J, Gedan K, Tully KL. The effects of saltwater intrusion on germination success of standard and alternative crops. *Environ Exp Bot*. 2020. <https://doi.org/10.1016/j.envexpbot.2020.104254>. 1;180.
29. Bradstreet RB. Kjeldahl method for organic nitrogen. *Anal Chem*. 1954;1(1):185–7.
30. Murphy J, Riley JP. A modified single solution method for the determination of phosphate in natural waters. *Anal Chim Acta*. 1962;1:27:31–6. [https://doi.org/10.1016/S0003-2670\(00\)88444-5](https://doi.org/10.1016/S0003-2670(00)88444-5).
31. Heiri O, Lotter AF, Lemcke G. Loss on ignition as a method for estimating organic and carbonate content in sediments: reproducibility and comparability of results. *J Paleolimnol*. 2001;25:101–10.
32. Mehlich A. Mehlich 3 soil test extractant: A modification of Mehlich 2 extractant. *Commun Soil Sci Plant Anal*. 1984;15(12):1409–16. <https://doi.org/10.1080/00103628409367568>.
33. Bates D, Mächler M, Bolker B, Walker S. Fitting linear mixed-effects models using lme4. *J Stat Softw*. 2015;7:67:1–48. <https://doi.org/10.18637/jss.v067.i01>.
34. Box GEP, Cox DR. An Analysis of Transformations. *Stat Soc Ser JR, Methodol B*. 1964; 1;26(2):211–43. <https://doi.org/10.1111/j.2517-6161.1964.tb00553.x>.
35. R Core Team 2020 R. A Language and Environment for Statistical Computing. R Foundation for Statistical Computing, Vienna, Austria. Available at <https://www.R-project.org/>. (Accessed April 2025).
36. USDA-NASS. Crop production summary, United States Department of Agriculture, National Agricultural Statistics Service. 2023. Available at <https://www.nass.usda.gov/Publications/>. (Accessed March 2025).
37. Miller JO, Adkins J. Monitoring winter wheat growth at different heights using aerial imagery. *Agron J*. 2021;113(2):1586–95. <https://doi.org/10.1002/agj2.20539>.
38. Corwin DL. Climate change impacts on soil salinity in agricultural areas. *Eur J Soil Sci*. 2021;72(2):842–62. <https://doi.org/10.1111/ejss.13010>.
39. Tanji KK, Kielen NC. Agricultural drainage water management in arid and semi-arid areas. Food and Agriculture Organization of the United Nations; 2002.
40. Tu M, Du C, Yu B, Wang G, Deng Y, Wang Y, et al. Current advances in the molecular regulation of abiotic stress tolerance in sorghum via transcriptomic, proteomic, and metabolomic approaches. *Front Plant Sci*. 2023. <https://doi.org/10.3389/fpls.2023.1147328>. 10;14:.
41. Yahaya MA, Shimelis H, Nebié B, Mashilo J, Pop G. Response of African sorghum genotypes for drought tolerance under variable environments. *Agronomy*. 2023;13(2):557. <https://doi.org/10.3390/agronomy13020557>.

42. Zheng H, Dang Y, Diao X, Sui N. Molecular mechanisms of stress resistance in sorghum: implications for crop improvement strategies. *J Integr Agric*. 2024;1(3):741–68. <https://doi.org/10.1016/j.jia.2023.12.023>.
43. Epanchin-Niell RS, Thompson A, Han X, Post J, Miller J, Newburn D et al. Coastal agricultural land use response to sea level rise and saltwater intrusion. 2023.
44. Adegoye GA, Olorunwa OJ, Alsajri FA, Walne CH, Wijewardana C, Kethireddy SR, et al. Waterlogging effects on soybean physiology and hyperspectral reflectance during the reproductive stage. *Agriculture*. 2023;4844. <https://doi.org/10.3390/agriculture13040844>.
45. Rhine MD, Stevens G, Shannon G, Wrather A, Slepser D. Yield and nutritional responses to waterlogging of soybean cultivars. *Irrig Sci*. 2010;1(2):135–42. <https://doi.org/10.1007/s00271-009-0168-x>.
46. Bai J, Gao H, Xiao R, Wang J, Huang C. A review of soil nitrogen mineralization as affected by water and salt in coastal wetlands: issues and methods. *CLEAN– Soil Air Water*. 2012;40(10):1099–105. <https://doi.org/10.1002/clean.201200055>.
47. Rath KM, Rousk J. Salt effects on the soil microbial decomposer community and their role in organic carbon cycling: A review. *Soil Biol Biochem*. 2015;1:81:108–23. <https://doi.org/10.1016/j.soilbio.2014.11.001>.
48. Burgin AJ, Hamilton SK. Have we overemphasized the role of denitrification in aquatic ecosystems? A review of nitrate removal pathways. *Front Ecol Environ*. 2007;5(2):89–96. [https://doi.org/10.1890/1540-9295\(2007\)5\[89:HWOTRO\]2.0.CO;2](https://doi.org/10.1890/1540-9295(2007)5[89:HWOTRO]2.0.CO;2).
49. Helton AM, Ardón M, Bernhardt ES. Thermodynamic constraints on the utility of ecological stoichiometry for explaining global biogeochemical patterns. *Ecol Lett*. 2015;18(10):1049–56. <https://doi.org/10.1111/ele.12487>.
50. Ardón M, Morse JL, Colman BP, Bernhardt ES. Drought-induced saltwater incursion leads to increased wetland nitrogen export. *Glob Change Biol*. 2013;19(10):2976–85. <https://doi.org/10.1111/gcb.12287>.
51. Weissman D, Ouyang T, Tully KL. Saltwater intrusion affects nitrogen, phosphorus and iron transformations under oxic and anoxic conditions: an incubation experiment. *Biogeochemistry*. 2021;1(3):451–69. <https://doi.org/10.1007/s10533-021-00796-6>.
52. Hartzell JL, Jordan TE. Shifts in the relative availability of phosphorus and nitrogen along estuarine salinity gradients. *Biogeochemistry*. 2012;107(1):489–500. <https://doi.org/10.1007/s10533-010-9548-9>.
53. Patrick WH, Khalid RA. Phosphate release and sorption by soils and sediments: effect of aerobic and anaerobic conditions. *Science*. 1974;186(4158):53–5. <https://doi.org/10.1126/science.186.4158.53>.
54. Carpenter SR. Phosphorus control is critical to mitigating eutrophication. *Proc Natl Acad Sci*. 2008;12(32):11039–40. <https://doi.org/10.1073/pnas.0806112105>.
55. Lucas E, Kennedy B, Roswall T, Burgis C, Toor GS. Climate change effects on phosphorus loss from agricultural land to water: A review. *Curr Pollut Rep*. 2023;1(4):623–45. <https://doi.org/10.1007/s40726-023-00282-7>.
56. Lan J, Liu P, Hu X, Zhu S. Harmful algal blooms in eutrophic marine environments: causes, monitoring, and treatment. *Water*. 2024;16(17):2525. <https://doi.org/10.3390/w16172525>.
57. de Barros PR, Schulenburg AN, Gedan K, Miller C, Tully KL. Effects of saltwater intrusion on candidate restoration species in coastal agricultural fields. *Agric Ecosyst Environ*. 2025;15:392:109757. <https://doi.org/10.1016/j.agee.2025.109757>.

Publisher's note

Springer Nature remains neutral with regard to jurisdictional claims in published maps and institutional affiliations.